Available online at www.sciencedirect.com
ScienceDirect
Nuclear Physics A 00 (2018) 1–4
Nuclear Physics A
www.elsevier.com/locate/procedia

XXVIIth International Conference on Ultrarelativistic Nucleus-Nucleus Collisions
(Quark Matter 2018)

Multiplicity dependence of strangeness and hadronic resonance production in pp and p-Pb collisions with ALICE at the LHC

Ajay Kumar Dash (For the ALICE collaboration)

School of Physical Sciences, National Institute of Science Education and Research, HBNI, Jatni-752050, India

Abstract

One of the key results of the LHC Run 1 was the observation of an enhanced production of strange particles in high multiplicity pp and p–Pb collisions at $\sqrt{s_{\rm NN}}$ = 7 and 5.02 TeV, respectively. The strangeness enhancement is investigated by measuring the evolution with multiplicity of single-strange and multi-strange baryon production relative to non-strange particles. A smooth increase of strange particle yields relative to the non-strange ones with event multiplicity has been observed in such systems. We report the latest results on multiplicity dependence of strange and multi-strange hadron production in pp collisions at $\sqrt{s}$ = 13 TeV with ALICE. We also presented recent measurements of mesonic and baryonic resonances in small collision systems like pp and p–Pb at $\sqrt{s_{\rm NN}}$ = 13 and 8.16 TeV, respectively. The system size dependent studies in pp and p-Pb collisions have been used to investigate how the hadronic scattering processes affect measured resonance yields and to better understand the interplay between canonical suppression and strangeness enhancement. The measurement of the $\phi(1020)$ meson as a function of multiplicity provides crucial constraints in this context.

Keywords: strangeness enhancement, hadronic phase, re-scattering

1. Introduction

The enhancement of strangeness production in high-energy nucleus-nucleus collisions (A–A) relative to the production in proton-proton (pp) collisions has historically been proposed as one of the signatures of Quark-Gluon Plasma (QGP) formation [1]. Experimentally, this was first observed in Pb–Pb collisions at SPS [2] and subsequently at RHIC [3] and LHC [4]. This enhancement in A–A collisions has also been explained as a suppression of strangeness production in reference samples like pp and p–Pb due to the lack of phase space for strange quark creation in small systems [5]. Recently, the ALICE Collaboration has observed that the yields of strange hadrons are enhanced relative to non-strange hadrons in high multiplicity pp collisions at $\sqrt{s}$ = 7 TeV and the strangeness enhancement in high multiplicity pp collisions reaches the values observed in p-Pb and peripheral PbPb collisions [6]. The strength of this enhancement increases with increasing strange quark content of the hadron. It was observed that the enhancement of strangeness production in small systems is due to the strangeness content rather than mass or a meson-baryon effect. As

the net strangeness of ϕ-meson is zero, it is interesting to study how the ϕ-meson behaves in the strangeness enhancement picture. It has been observed that by comparing similar event multiplicity and by changing the colliding system (pp, p–Pb and Pb–Pb) the relative particles abundances are not modified. By comparing the results from the pp collisions at $\sqrt{s}$ = 13 TeV to those at lower energies, the center-of-mass energy dependence of hadrochemistry can be isolated. It is also interesting to measure the short-lived resonance particles like K^{*0} ($\tau \sim 4.2$ fm/c) and ϕ ($\tau \sim 46.3$ fm/c). These hadrons may decay during the hadronic phase (phase between chemical and kinetic freeze-out). As a result, the decay daughters may re-scatter, leading to a reduction in the measurable resonance yields. They may also be regenerated due to pseudo-elastic scattering of hadrons through a resonance state, which enhances their production [7]. The centrality or multiplicity dependent suppression of the K^{*0}/K ratio has been observed in p–Pb and Pb–Pb collisions [8, 9]. So, it is most important to see if such an effect can be observed in high-multiplicity pp collisions, which might be an indication for a hadronic phase with non-zero lifetime. In this work, we present the multiplicity dependence of resonance, strange and multi-strange hadron production in pp and p–Pb collisions measured with the ALICE detector at $\sqrt{s_{\rm NN}}$ = 13 and 8.16 TeV, respectively.

2. Analysis

A detailed description of the ALICE apparatus can be found in ref. [10]. The main detectors which are relevant to this analysis are the Time Projection Chamber (TPC), the Time-of-Flight detector (TOF), the Inner tracking system (ITS) (covering the mid-rapidity window of $|\eta| < 0.9$) , and the V0 (V0A covering $2.8 < \eta < 5.1$ and V0C covering $-3.7 < \eta < -1.7$) detector. The multiplicity classes are defined based on percentiles of the distribution of the summed amplitudes measured in the V0 detectors (V0A+V0C) [11]. The measurements of resonance, strange and multi-strange hadron production are performed at mid-rapidity ($|y| < 0.5$ in pp collisions and $0 < y_{cm} < 0.5$ in p-Pb collisions) as a function of the charged particle density, which is also measured at mid-rapidity for each multiplicity class. The aforementioned measurements are performed via the invariant mass analysis based on the following decay channels (branching ratios): $K^{*0}(\bar{K}^{*0}) \rightarrow K^+\pi^-(K^-\pi^+)$ (66.6 %), $\phi \rightarrow K^+K^-$ (48.2 %), $K^0_S \rightarrow \pi^+\pi^-$ (69.2%), $\Lambda \rightarrow p\pi^-$ (63.9%), $\Xi \rightarrow \Lambda\pi^-$ (99.9%) and $\Omega \rightarrow \Lambda K^-$(67.8%). In the invariant-mass method one needs to estimate the combinatorial background, which is evaluated by using an event-mixing technique for resonances. For strange and multi-strange hadrons, a set of topological cuts is applied to eliminate the candidates which do not fit the expected decay topology. After the background subtraction the raw yields are extracted from the signal distribution to be then corrected for detector acceptance, tracking efficiency and branching ratio. The first two corrections were determined by means of Monte Carlo simulations of the ALICE detector response.

3. Results and discussion

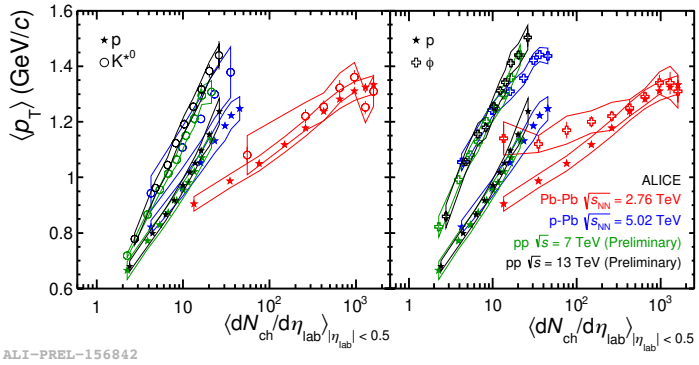

Fig. 1. (Color online) Mean transverse momentum ($\langle p_{\rm T} \rangle$) of K^{*0}, ϕ and p in pp (at $\sqrt{s}$ = 7 and 13 TeV), p–Pb (at $\sqrt{s_{\rm NN}}$ = 5.02 TeV) and Pb-Pb (at $\sqrt{s_{\rm NN}}$ = 2.76 TeV) collisions as functions of multiplicity. The bars represent the statistical error and the lines represents the systematic error.

The production of K^{*0}, ϕ, K^0_S, Λ, Ξ and Ω is measured in different multiplicity classes in pp collisions at $\sqrt{s}$ = 13 TeV in a wide $p_{\rm T}$ range. In addition, the resonances are also measured in several multiplicity classes in p–Pb collisions at $\sqrt{s_{\rm NN}}$ = 8.16 TeV. The $p_{\rm T}$ integrated hadron yields (dN/dy) and mean $p_{\rm T}$ ($\langle p_{\rm T} \rangle$) for each multiplicity event class are determined by integrating the $p_{\rm T}$ spectra in the measured range and by using

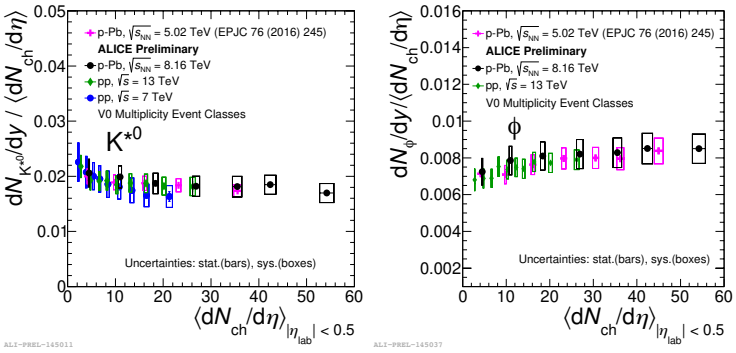

Fig. 2. (Color online) Integrated yields of K^{*0} (left panel) and ϕ (right panel) normalized to $\langle dN_{ch}/d\eta \rangle$ in pp collisions (at $\sqrt{s}$ = 7 and 13 TeV) and p–Pb collisions (at $\sqrt{s_{NN}}$ = 5.02 and 8.16 TeV) for different multiplicity classes. The bars and the boxes represent the statistical and systematic error, respectively.

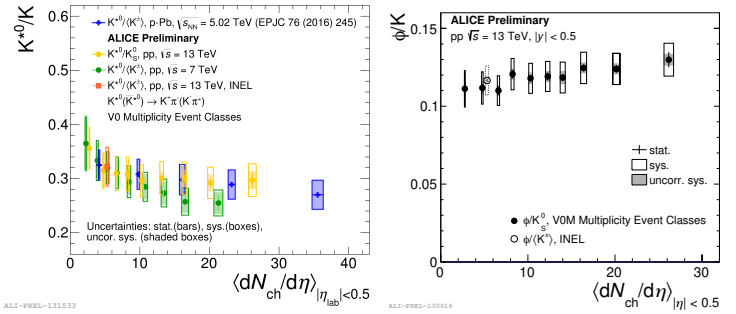

Fig. 3. (Color online) Ratios of the integrated yields, K^{*0}/K (left panel) measured in pp collisions at $\sqrt{s}$ = 7 and 13 TeV and p–Pb collisions at $\sqrt{s_{NN}}$ = 5.02 and 8.16 TeV and ϕ/K (right panel) in pp collisions at $\sqrt{s}$ = 13 TeV for different multiplicity classes. The bars and the boxes represent the statistical and systematic error, respectively.

a Lévy-Tsallis fit function to extrapolate the yields in the unmeasured p_T region. Figure 1 shows the $\langle p_T \rangle$ of K^{*0}, ϕ and proton as a function of the average charged particle multiplicity density ($\langle dN_{ch}/d\eta \rangle$) measured at mid-rapidity ($|y| < 0.5$) in pp collisions at $\sqrt{s}$ = 13 TeV and compared with the results obtained in pp, p–Pb and Pb–Pb collisions at $\sqrt{s_{NN}}$ = 7, 5.02 and 2.76 TeV, respectively. For all the particles studied an increase in $\langle p_T \rangle$ from low to high multiplicity classes is observed. The same increasing trend of the $\langle p_T \rangle$ as a function of the multiplicity is observed in pp collisions at $\sqrt{s}$ = 7 TeV and 13 TeV and a mass ordering of $\langle p_T \rangle$ is found to be followed in central and semi-central Pb–Pb collisions, i.e., particles with similar masses have similar $\langle p_T \rangle$ values, as expected from the hydrodynamic expansion of the system [12]. However, this breaks down for smaller systems. The increase in $\langle p_T \rangle$ is steeper for smaller systems. The yields normalized to the $\langle dN_{ch}/d\eta \rangle$ of $K^{*0}$and ϕ in pp collisions at $\sqrt{s}$ = 7 and 13 TeV, p-Pb collisions at $\sqrt{s_{NN}}$ = 5.02 and 8.16 TeV are shown as a function of multiplicity in Fig. 2. It is observed that at similar multiplicity, particle production is independent of the system size and collision energy. The yield ratios of resonances to long lived hadrons as a function of $\langle dN_{ch}/d\eta \rangle$ for pp collisions at $\sqrt{s}$ = 7 and 13 TeV and p–Pb collisions at $\sqrt{s_{NN}}$ = 5.02 TeV are shown in Fig. 3. The ratio ϕ/K , $\Sigma^{*\pm}/\Lambda$ (not shown here) and Λ^{*}/Λ (not shown here) are independent of the event multiplicity in pp and p-Pb, consistent with re-scattering/re-generation effects. A hint of a decrease in the K^{*0}/K^{0}_{S} ratio is seen from low to high multiplicity pp and p–Pb collisons, which might be

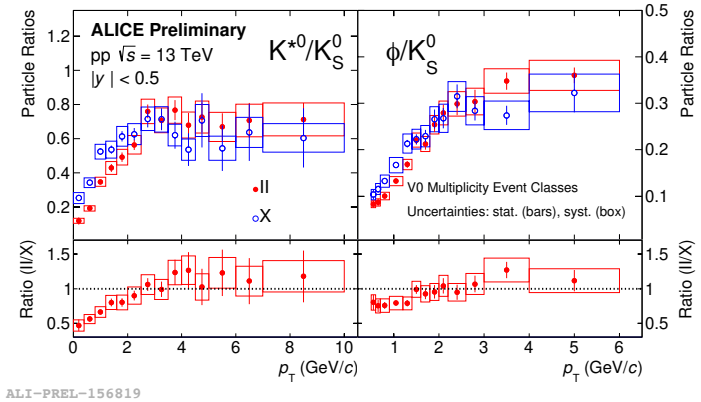

Fig. 4. (Color online) p_T differential ratio of K^{*0}/K^{0}_{S} (left panel) and ϕ/K^{0}_{S} (right panel) in pp collisions at $\sqrt{s}$ = 13 TeV for two different extreme multiplicity classes, where the $\langle dN_{ch}/d\eta \rangle$ in high (II) and low (X) multiplicity classes are ~ 20 and 2.4, respectively. The bottom panel shows the ratio between the yield ratio in high to low multiplicity class. The bars and the boxes represent the statistical and systematic error, respectively.

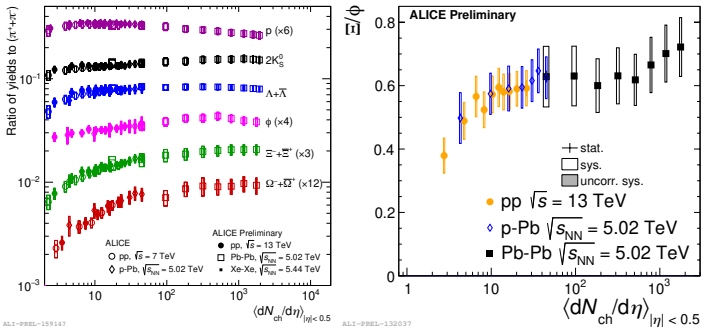

Fig. 5. (Color online) Left panel: Ratios of the integrated yields, $(p+\bar{p})/(\pi^+ + \pi^-)$, $2K^0_S/(\pi^+ + \pi^-)$, $(\Lambda + \bar{\Lambda})/(\pi^+ + \pi^-)$, $2\phi/(\pi^+ + \pi^-)$, $(\Xi + \bar{\Xi})/(\pi^+ + \pi^-)$, $(\Omega + \bar{\Omega})/(\pi^+ + \pi^-)$, measured as a function of the charged particle density in pp (at $\sqrt{s}$ = 7 and 13 TeV), p–Pb (at $\sqrt{s_{NN}}$ = 5.02 TeV) and Pb-Pb (at $\sqrt{s_{NN}}$ = 5.02 TeV) collisions. Right panel: Ratios of the integrated yields, $(\Xi + \bar{\Xi})/\phi$ in pp collisions at $\sqrt{s}$ = 13 TeV, p–Pb and Pb-Pb collisions at $\sqrt{s_{NN}}$ = 5.02 TeV. The bars and the boxes represent the statistical and systematic error, respectively.

due to re-scattering. As re-scattering is important at low p_T, we looked into the p_T differential ratios K^{*0}/K^0_S and ϕ/K^0_S, which are shown in Fig. 4 for two extreme multiplicity classes, K^{*0}/K^0_S in the left panel and ϕ/K^0_S in the right panel. In the bottom panels the ratios of high to low multiplicity classes are shown. Both ratios increase at low p_T and saturate for $p_T > 3$ GeV/c. Depletion in the ratios for high multiplicity at low p_T is observed. From the bottom panels it is clear that the K^{*0}/K^0_S ratio is more suppressed compared to ϕ/K^0_S for $p_T < 2$ GeV/c. This observation is consistent with a re-scattering effect in high multiplicity pp collisions. The ratio of particle yields to pions as a function of $\langle dN_{ch}/d\eta \rangle$ in pp at $\sqrt{s}$ = 7 and 13 TeV, p–Pb and Pb-Pb at $\sqrt{s_{NN}}$ = 5.02 TeV is shown in the left panel of Fig. 5. The ratios from pp collisions at $\sqrt{s}$ = 13 TeV are in agreement with the measurement at lower energy. A smooth transition is observed between pp, p-Pb and Pb-Pb: at similar multiplicity strangeness production is independent of collision system and energy. The ϕ also shows strangeness enhancement from low to high multiplicity. The ratios ϕ/K^0_S and Ξ/ϕ (shown in the right panel of Fig. 5 for pp collisions at $\sqrt{s}$ = 13 TeV and p–Pb and Pb–Pb collisions at $\sqrt{s_{NN}}$ = 5.02 TeV) show a flat or slowly increasing trend over a wide range of multiplicity. This suggests that the ϕ behaves like a particle with effective strangeness between 1 and 2, similar to K and Ξ. This is important, since ϕ is not subject to canonical suppression, whereas K and Ξ should be canonically suppressed.

4. Summary

The ALICE collaboration reported results on resonance, strange and multi-strange particle production as a function of multiplicity in pp and p–Pb collisions at $\sqrt{s_{NN}}$ = 13 and 8.16 TeV, respectively. Measurements of particle spectra at different energies as a function of multiplicity indicate that the hadrochemistry is rather driven by event multiplicity than by system size to collision energy. A hint of a decrease is observed for the p_T-integrated K^{*0}/K^0_S ratio from low to high multiplicity pp and pPb collisions, while ϕ/K^0_S ratio remains constant. Those observations suggest the presence of re-scattering effects in high multiplicity pp collisions. Like other strange hadrons, the ϕ shows strangeness enhancement from low to high multiplicity class in pp collisions and behaves like a particles with net strangeness between 1 and 2. The strangeness enhancement depends on the strangeness content of the particle.

References

[1] J. Rafelski and B. Muller, Phys. Rev. Lett. 48, (1982) 1066. [Erratum: Phys. Rev. Lett. 56, (1986) 2334].
[2] E. Andersen et al. Phys. Lett. B 449, (1999) 401406. F. Antinori et al. (NA57 Collaboration), J. Phys. G 32, (2006) 427.
[3] B. I. Abelev et al. (STAR Collaboration) Phys. Rev. C 77, (2008) 044908.
[4] B. Abelev et al. (ALICE Collaboration) Phys. Lett. B 728, (2014) 216.
[5] A. Tounsi, A. Mischke and K. Redlich, Nucl. Phys. A 715, (2003) 565.
[6] J. Adam et al. (ALICE Collaboration) Nature Physics 13, (2017) 5359.
[7] S. A. Bass and A. Dumitru, Phys. Rev. C 61, (2000) 064909.
[8] J. Adam et al. (ALICE Collaboration) Eur. Phys. J. C 76, (2016) 245.
[9] J. Adam et al. (ALICE Collaboration) Phys. Rev. C 95, (2017) 064606.
[10] K. Aamodt et al. (ALICE Collaboration) J. Inst. 3, (2008) No. S08002 i245.
[11] B. Abelev et al. (ALICE Collaboration) Phys. Rev. C 88, (2013) 044909.
[12] C. Shen, U. Heinz, P. Huovinen, and H. Song, Phys. Rev. C 84, (2011) 044903.